THE ASTROPHYSICAL JOURNAL, 369:13–19, 1991 March 1

CLUSTER INFALL WITH FRICTION

R. G. CARLBERG AND JOHN DUBINSKI
Department of Astronomy, University of Toronto, Toronto, Ontario, Canada M5S 1A1
Received 1990 June 8; accepted 1990 August 20

ABSTRACT

Cluster formation via cosmological infall of correlated galaxies is mildly dissipative in the sense that dynamical friction resists the motion of mass concentrations through the background density field. As the galaxies fall into the cluster, their dark halos are tidally disrupted, effectively terminating friction in high-velocity dispersion clusters. The galaxy population in clusters is therefore predicted to be dynamically cooler than the purely dissipationless dark matter component, and should have a correspondingly steeper density profile. A completely dissipationless n-body simulation of the formation of a cluster of galaxies explicitly demonstrates that the high-density central regions of galaxy-size dark halos which are present prior to the formation of a virialized cluster remain a statistically distinct population in the cluster. The ratio of the average radial velocity dispersions of the galaxy tracer population, σ_*, to those of the dark matter, σ_ρ, remains fairly stable around $b_{vr} = \sigma_*/\sigma_\rho = 0.8$. The galaxy tracer population is in better accord with the density profile of galaxies in clusters than the approximately isothermal dark matter population. The presence of a dynamically cool galaxy population in the relatively low-friction environment of a cluster reinforces the fact that the velocity dispersions of galaxies always underestimate those of the general density field, and strongly suggests that $b_v < 0.8$ in the field.

Subject headings: cosmology — galaxies: clustering — galaxies: interactions

1. INTRODUCTION

Galaxies are regions of high density containing a small fraction of the uncertain total mass density of the universe and are likely to be biased tracers of both clustering and dynamics in the universe (e.g., Kaiser 1984; White et al. 1987; Carlberg, Couchman, & Thomas (1990). The possibility of reconciling the dynamically estimated values of Ω that indicate an open universe with the flat universe expected from an inflationary cosmology is a considerable attraction of bias. The clustering of galaxies can either be enhanced or reduced with respect to the dark matter background by statistical effects (e.g., Kaiser 1984; Carlberg 1991) and increased by dynamical evolution (e.g., Barnes 1984; Evrard 1986; West & Richstone 1988). Current observations confine b_ρ, the ratio of density contrasts in the galaxy distribution to those in the dark matter, to a range $1 \lesssim b_\rho \Omega^{-0.6} \lesssim 2.5$, (Lynden-Bell et al. 1988; Evrard 1989; Peebles, Daly, & Juskiewicz 1989; Kaiser & Lahav 1989; Lynden-Bell, Lahav & Burstein 1989; Frenk et al. 1990), with analyses of large-scale flow velocities favoring lower values and a variety of techniques suggesting values around $b_\rho \Omega^{-0.6} \simeq 1.5$. A clustering of this size is not sufficient to raise the dynamically inferred Ω to unity.

Dynamical friction resists the motion of galaxies as they move through the surrounding dark matter, and therefore generally acts to cool the galaxy velocities, σ_*, in comparison to those in the density field, σ_ρ, leading to a velocity dispersion bias, $b_v = \sigma_*/\sigma_\rho \leq 1$ (Carlberg et al. 1990). The evidence for a b_v substantially smaller than unity is, at present, limited to cosmological n-body simulations (Carlberg & Couchman 1989; Carlberg 1991), and is subject to the substantial uncertainty in the origin of galaxies. The importance of dynamical friction on galaxy orbits in small groups is well-established (Barnes 1984. 1985; Evrard 1986, 1987; West & Richstone 1988). If a group is left in isolation, the orbit decay inevitably leads to a rapid merging and destruction of the individual galaxies. On the other hand, galaxies in large clusters are expected to lose their individual dark halos, so that, once they have come into equilibrium, dynamical friction has a relatively small effect on orbital velocities (e.g., White 1976; Richstone & Malamuth 1983; Merritt 1987; Lauer 1988).

The cosmic virial theorem (CVT; Peebles 1976) estimate of Ω is directly proportional to the square of the pairwise velocity dispersion in the matter field. These velocities are created by the pattern of clustering and are therefore weighted towards the velocities in the relatively abundant groups and loose clusters. If velocity bias is to be a significant effect which leads galaxies to underestimate Ω, galaxies in clusters must have lower orbital velocities than the underlying dark matter density field, even though both populations are in equilibrium with the cluster potential, and the galaxies are no longer greatly affected by dynamical friction. This paper establishes that the high-density regions of the dark halos present prior to cluster collapse, that is, the likely sites of galaxies, form a statistically distinct, dynamically cool population within the cluster. An important consequence is that the ratio of galaxy velocity dispersions in clusters to the dark matter velocity dispersion sets an upper limit on the value of the velocity bias for the entire field.

A completely dissipationless N-body experiment that has sufficient resolution to follow the internal dynamics of the many galaxy-size dark halos that eventually make the cluster is presented in the next section. This allows galaxy tracers to be identified as the high-density regions of the galaxy-scale halos present prior to cluster formation. The largest cluster in the simulation is measured in § 3 and found to have a $b_{vr} \simeq 0.8$ in the radial velocity dispersion with a galaxy population in better accord with cluster observations than the dark matter distribution. Comparison in § 4 of the energy history of infalling material shows that the dense cores of dark halos, where galaxies are located, lose energy approximately as expected for dynamical friction terminated by tidal disruption.

2. A NUMERICAL CLUSTER OF GALAXIES

There are two important conditions that are extremely desirable for a cosmologically realistic cluster n-body simulation. First, if galaxies are represented by particles more massive than those representing the dark matter, dynamical friction between the two is inevitable, and two-body relaxation in small units is a strong possibility. We minimize these difficulties by using a single particle mass for both the galaxy tracers and the dark matter, and concentrate many particles into the region of a cluster to increase the resolution. Having a single particle mass and no dissipation likely leads to an underestimate of the mass of galaxies and, if anything, suppresses the dynamical friction which is important in creating velocity bias. As such this is useful in establishing the cause as being primarily associated with the large mass in the correlated halos of galaxies. The second condition is that the numerical model of the cluster must be consistent with a cosmology which matches the basic galaxy-galaxy correlation function, pairwise velocity measurements, and number density of galaxies. If the galaxies are restricted in their ability to build up correlated dark halos, then the friction effects are negligible (West & Richstone 1988). In the absence of a proper match to the field correlation function, the friction effects could either be under- or overestimated. To achieve consistency with a normalized cosmological model, we evolve a small region scooped out of a large cosmological model which has previously been shown to meet the basic constraints.

In the following discussion, the background cosmology is assumed to have $\Omega = 1$, containing a CDM spectrum of density fluctuations. Scaling is done assuming $H_0 = 50$ km s^{-1} Mpc^{-1}. The largest peak identified with a 5 Mpc Gaussian filter is taken as the center of a 10 Mpc sphere for the cluster simulation. The total mass of this region, in the absence of perturbations, is $2.90 \times 10^{14}\ M_{\odot}$, and each of the 262,144 particles weighs $1.1 \times 10^9\ M_{\odot}$. The final cluster will have a line-of-sight velocity dispersion of about 500 km s^{-1}. This cluster is representative of the upper end of the velocity-dispersion range of groups and clusters found in the sample of relatively nearby galaxies which has been used for the CVT measurement (Davis & Peebles 1983; Ramella, Geller, & Huchra 1989). If the reader would prefer to match the results to Coma, an approximate model from a CDM cosmology can be had simply by multiplying all lengths and velocities by 2, and masses by 8.

CDM initial conditions (Bond & Efstathiou 1984) are created in a cube with edges 40 Mpc, on a 128^3 grid, using the same code as in Carlberg et al. (1990) and Carlberg (1991). The initial moment corresponds to $z = 9$ in an unbiased universe, with growing mode position and velocity perturbations given by the Zeldovich approximation. A sphere of particles 10 Mpc in diameter is scooped out around the highest peak, and the appropriate Hubble expansion velocity is added to convert the simulation to a calculation in physical units. The scooping-out procedure creates vacuum boundary conditions for the simulation, which will introduce large departures from the true cosmological dynamical behavior on the scale of the simulation. These large-scale discrepancies are not a difficulty, since the primary goal here is to study the dynamics of the substructure in comparison to the dark matter in the cluster, which is not expected to be strongly dependent on the large-scale structure outside of this cluster. The cluster at $z = 0$ will contain $\simeq 25\%$ of the particles, and exhibits the important basic feature of formation via the cosmological infall of "naturally" created substructure.

The positions, velocities, and masses are given to a tree-code n-body program (Barnes & Hut 1986) to evolve forward in time. The initial mean separation between particles is 25 kpc, the softening length is set to 15 kpc, the angular tolerance of the tree-code is set to 1, and quadrupole corrections are enabled. The time steps are fixed at 20 Myr each. Figure 1 shows the simulation at $z = 3$, with particles in $\rho/\rho_0 > 8000$ picked out. By $z = 0$ most of the material in the upper right will be incorporated into the single largest cluster in the simulation.

3. VELOCITIES AND DENSITIES

At $z = 0$ (normalized to a $b = 1$ CDM cosmology) the largest group of particles in the simulation is identified. This cluster, unsurprisingly, is close to another, somewhat smaller, cluster at a distance of 2.38 Mpc, with a mass 0.43 of the large one. The two clusters merge in another 2.4 Gyr. The kine-

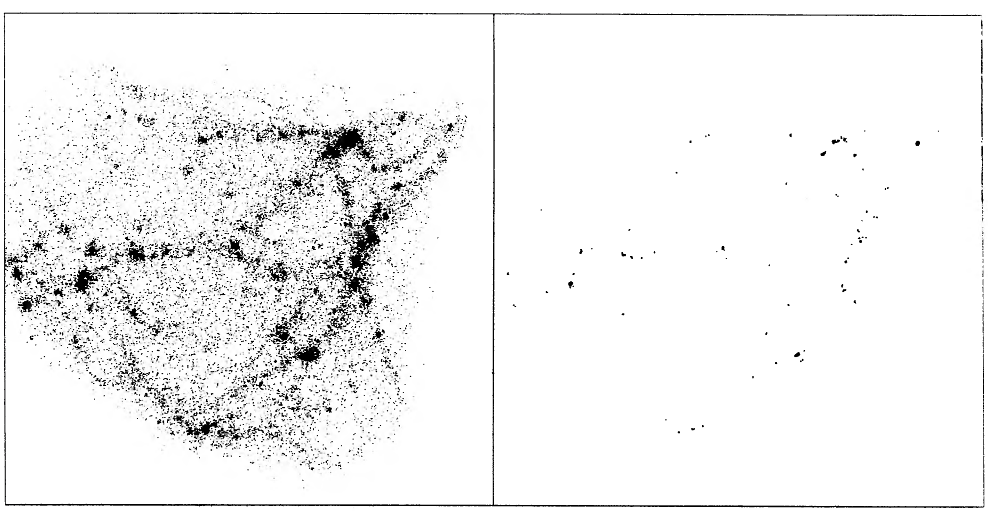

FIG. 1.—The x-y projection at $z = 3$ of $\frac{1}{8}$ of all the particles (*left panel*) and those particles in groups having $\rho/\rho_0 \geq 8000$ and containing at least 10 particles (*right panel*), which selects 4764 of the 262,144 particles. The box edge is 5 Mpc (comoving). Most of the groups in the upper right will merge to form the cluster.

matics and densities of the 58,247 particles within a 1.25 Mpc sphere centered on the large cluster are analyzed. At the outer edge of this sphere the dark matter density is approximately $100\rho_0$, and $\langle v_r \rangle/\sigma_r \simeq -0.1$, therefore the material analyzed is dominantly in the virialized region of the cluster.

The cluster is a fairly flat triaxial ellipsoid, but for the sake of simplicity and to emphasize the differences between the dark matter and the galaxy tracer population the following analysis will present quantities averaged on spherical shells. Only a small fraction, less than 10%, of particles will be identified as galaxy tracers, so the dark matter analysis includes all the mass inside the 1.25 Mpc sphere.

3.1. *Dark Matter*

The dark matter in the cluster is, to a low order of approximation, an isothermal, isotropic sphere, in marked contrast to the roughly r^{-3} or steeper profiles that are created in violent relaxation (e.g., van Albada 1982). The density profile, shown in Figure 2 as plus symbols, has approximately the form expected for cosmological infall (Gott & Gunn 1972; Gunn 1977; Filmore & Goldreich 1984; Bertschinger 1985), that is, a density profile slightly steeper than r^{-2}. The core radius of the dark matter distribution here is essentially equal to the softening radius. The velocity dispersion in the dark matter, Figure 3, declines slowly with radius (note the logarithmic density scale) dropping from about 500 km s^{-1} at 0.1 Mpc to 300 km s^{-1} at 1 Mpc. The velocity ellipsoid, Figure 4, has a modest radial elongation, $\sigma_\perp/\sigma_r$, drooping slightly from 0.90 near the center to 0.75 at the "virializing edge," about 1 Mpc from the center. The dark matter in the cluster is quite triaxial near the center (120:140:220 kpc principal axes), becoming more spherical outwards (650:760:910 kpc). In the center the velocity ellipsoids are aligned with the principal axes, becoming more radially aligned in the outer region.

3.2. *Galaxy Tracers*

Identifying suitable galaxy tracers in the dark matter of a dissipationless simulation is a problem without a clear solution at present. Galaxies are thought to form in the high-density

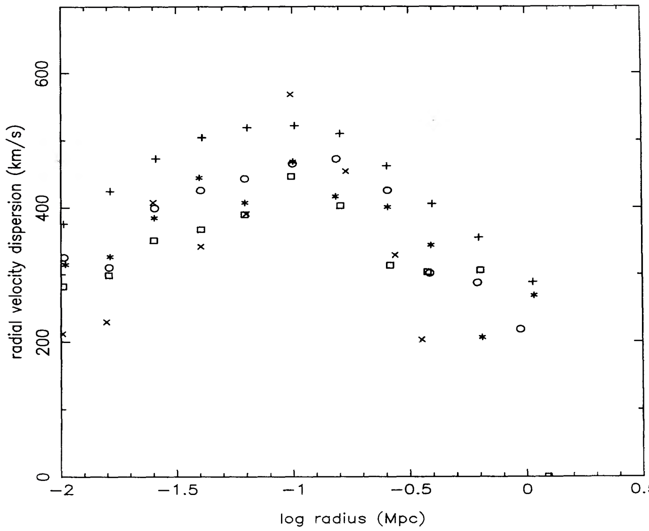

FIG. 3.—Velocity dispersion vs. radius for the same particles as in Fig. 2, with the same symbols; the particles (*plus symbols*), and the galaxy tracers identified at redshifts 3.84 (*crosses*), 3.0 (*stars*), 2.05 (*circles*), and 0.59 (*squares*).

centers of dark halos having total masses of approximately 10^{10}–10^{12} $M_\odot$ at some time prior to cluster collapse (White & Rees 1978). Picking out the particles in the central regions of halos present in the redshift range $1 \lesssim z \lesssim 4$ gives reasonable galaxy tracing particles. No merging between these galaxy tracers is allowed, although this is likely to be a small effect (see White et al. 1987), and in any case would only lower galaxy velocities further.

Galaxies are observed to be in regions having densities of order 10^5 times the critical density. The correlation function $\xi = (r/10 \text{ Mpc})^{1.8}$ gives, at 10 kpc, $\rho/\rho_0 = 7.2 \times 10^4$. For a galaxy with a rotation curve flat at v_c the density contrast at radius r is $\rho(r)/\rho_0 = 2\pi/3(v_c/Hr)^2$, which for $v_c = 200$ km s^{-1} is 3.4×10^5 at 10 kpc. The softening length here is 15 kpc, making such high overdensities difficult to realize, even with this relatively large high-resolution simulation. We will consider particles at $\rho/\rho_0 > 8000$ and 64,000 identified at $z \gtrsim 1$ as

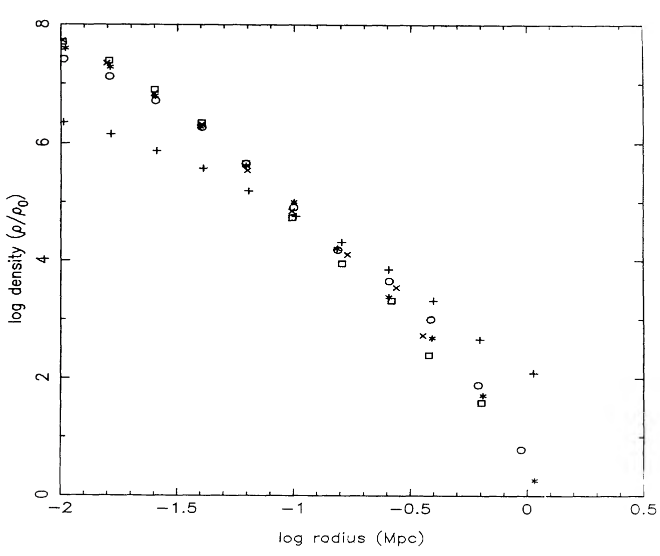

FIG. 2.—Density vs. radius for all the particles (*plus symbols*) and for particles identified in $\rho/\rho_0 > 8000$ regions at redshifts 3.84 (*crosses*), 3.0 (*stars*), 2.05 (*circles*), and 0.59 (*squares*).

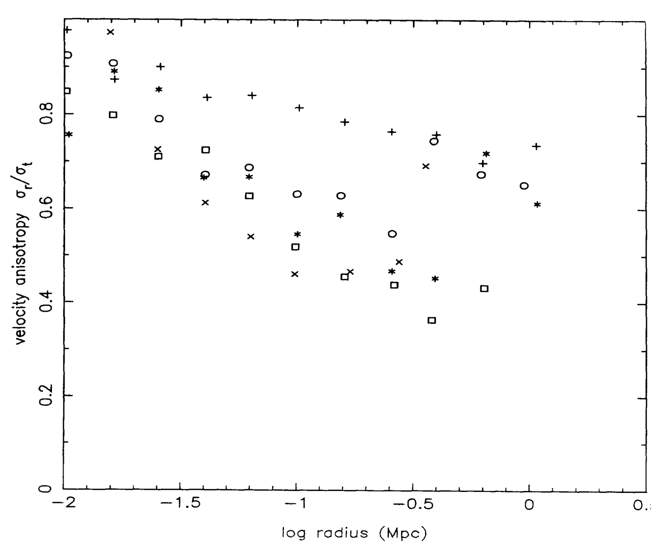

FIG. 4.—Velocity anisotropy vs. radius. The symbols have the same meaning as in Figs. 2 and 3.

suitable galaxy tracers. The particles at lower overdensities which surround these high-density regions are quickly stripped during cluster formation. By the end of simulation most particles in the dense central regions have also been tidally shredded, so the entire halo is dispersed over the cluster. N-body codes with more resolution will be able to test whether a small, dense core region is able to orbit freely in the cluster.

It will be assumed that galaxy orbits are statistically traced by the particles initially in the dense central regions of halos selected at higher redshifts. This identification removes the capacity of the "galaxy" itself to be subject to dynamical friction, and may therefore *overestimate* the velocities of galaxies in clusters. Similarly the central particles in the halo have the velocity dispersion of the halo, and therefore have somewhat higher kinetic energies than galaxies which are at rest with respect to the center of the halo. The galaxy tracers are found using a linking algorithm which builds a minimal spanning tree between the particles, then prunes the three into clumps at links longer than some specified value. For instance, a pruning length that is $\frac{1}{5}$ of the mean interparticle spacing of the uniform background implies the outer density contour of the clump is 125 times that in the background cosmology.

Figure 1 shows both the x-y projection of the positions of all the particles and those in groups that contain more than 10 particles with $\rho/\rho_0 \geq 8000$, identified at $z = 3$. The largest of these groups contains 363 particles, whereas the cluster at $z = 0$ will contain more than 50,000 particles.

Figure 2 shows that the $\rho/\rho_0 > 8000$ cores of dark halos identified at any $z \gtrsim 0.5$ have a steeper density profile than the dark matter. A satellite population at velocity dispersion σ_* in equilibrium in a singular isothermal potential characterized by a velocity dispersion σ_ρ has a power-law density distribution with slope $2(\sigma_\rho/\sigma_*)^2$. The radial velocity dispersions are shown in Figure 3, confirming that the galaxy population is shallower than the dark matter. As discussed below, the low-velocity dispersion is the result of energy loss from the halo centers, and the concentration of the galaxies to the cluster center is an inevitable consequence once the cluster comes into equilibrium. The data is plotted for a wider range of identification redshifts, showing that the velocity bias is not a sensitive function of the identification redshift, although there is a scatter of about 10% in the results, with the highest and the lowest redshifts giving lower velocity dispersions. Running the simulation forward to a 50% greater age does not significantly diminish the velocity bias, although the cluster mass does continue to grow, approximately at the $t^{2/3}$ rate.

The velocity ellipsoid of the galaxy population is significantly more radial than in the dark matter, as shown in Figure 4. The ratio $\sigma_\perp/\sigma_r$ declines from 0.85 near the center to 0.50 near the "virializing edge." This relatively modest decline is in marked contrast to the large radial anisotropy produced in violent relaxation experiments that create de Vaucouleurs-type density profiles (e.g., van Albada 1982; Tremaine 1987). The main difference of approach is that those experiments usually are "dropped," that is, the initial radial velocities are zero, rather than the perturbed Hubble flow used here. Initially expanding simulations build structure through a lumpy infall, having much smaller energy changes than during the violent relaxation of a dropped simulation.

The magnitude of the galaxy tracer dynamical cooling depends on the density used to select the galaxies, as shown in Table 1, where the ratio of the average σ_r and the full three-dimensional velocity dispersion in the galaxies to the dark matter is given for the halos identified at $z = 2.05$. Including the tangential components decreases the ratios, since the galaxy tracers have radially elongated velocity ellipsoids. Identifying galaxies with particles at densities $\rho \gtrsim 1000\rho_0$, gives greatly reduced effects, and the "just virialized" density of $\rho \geq 120\rho_0$ includes approximately 50% of the mass and traces the dark matter density field quite accurately. Regions at densities greater than $64{,}000\rho_0$ are only marginally resolved and have poor statistics, but appear to give a further decrease in the population radial velocity dispersion, to 0.78 of the dark matter value.

TABLE 1

DENSITY DEPENDENCE OF COOLING

$\rho > \delta\rho_0$, $\delta =$	Number	$\langle\sigma_*/\sigma_\rho\rangle_r$	$\langle\sigma_*/\sigma_\rho\rangle_{3D}$
1	58247	1.00	1.00
125	33826	0.97	0.95
1000	16922	0.93	0.91
8000	3269	0.85	0.78
64000	150	0.77	0.62

The ratios of galaxy to dark matter velocity dispersion, σ_*/σ_ρ at $\rho > 8000\rho_0$ ranges from 0.70 to 0.90, with an average value of 0.85, using the data shown in Figure 2. The decrease in both the radial b_{vr} and the full b_v shown in Table 1 suggests that a conservative estimate of b_{vr} at the overdensities of galaxies is 0.8, and that b_v is about 5%–10% less. The most statistically reliable number in Table 3 which is at a reasonable overdensity is $b_v = 0.78 \pm 0.02$ for the $\delta = 8000$ tracers identified at $z = 3$. This paper is intended to provide a useful value for studying cluster dynamics, which in equilibrium tends to emphasize the radial dispersion, and a secure upper limit for the field value of the velocity bias. Based on the data of Figure 2 and Table 1, we therefore adopt $b_v = 0.8$. A small extra cooling would be introduced if galaxies were started at rest in their halos, if the friction on the self-gravitating luminous component was included, and if galaxies were allowed to merge.

4. DISSIPATIVE COSMOLOGICAL INFALL

Analytic discussions of cosmological infall assume that energy is conserved for individual mass points, which can be tested with the simulation data. The entire simulation is of course energy conserving, to better than 0.5% over the course of the run. The mean energies of the halos identified by the linking algorithm can be compared when they are distinct entities, and again after they have fallen into the cluster and are tidally shredded. Examining all material in halos with $\rho/\rho_0 \geq 125$ that fall into the cluster, we find that there is very little change in the average binding energy. At $z = 3$ the mean binding energy of these low-density halos with respect to the entire finite simulation is $(877 \text{ km s}^{-1})^2$, and at $z = 0$ the binding energy of these low-density halos is unchanged, within the accuracy of the measurement. We conclude that, to a good approximation, the bulk of the matter is energy-conserving during infall, and is tidally shredded before dynamical friction can play a significant role.

The particles in the high-density ($\rho/\rho_0 \geq 8000$) cores of the halos do not conserve energy. Their $z = 3$ binding energies are $(1193 \text{ km s}^{-1})^2$, rising to $(1325 \text{ km s}^{-1})^2$ at $z = 0$. The increase in binding energy is consistent with a simple model where the infalling orbits of the halos are slowed by dynamical friction until the halos are tidally disrupted. The cluster density profiles is approximately isothermal, $\rho(r) = \rho_0 r_c^2 r^{-2}$, with an equilibrium one-dimensional isothermal velocity dispersion of $\sigma_\rho^2 = 2\pi G \rho_0 r_c^2$. A galaxy that falls into this potential will initially have its own attached halo, $\rho_s(r) \simeq \rho_0 r_s^2 r^{-2}$, gradually removed. The effective mass of the infalling galaxy is dominated by the amount of correlated halo that is left at any time. The satellite halos will, on the average, be described by the correlation function. If the friction is strong enough, then the infall velocity of the satellite, v_s, approaches a terminal value,

$$\frac{v_s}{\sigma_\rho} \simeq \frac{3}{2 \ln \Lambda} \sqrt{\frac{\pi}{2}} \left(\frac{\sigma_\rho}{\sigma_s}\right)^2 , \tag{1}$$

where σ_s is the internal velocity dispersion of the satellite halo. The original derivation of this equation (Carlberg 1991) assumed that $\sigma_s = \sigma_\rho$. For the satellites measured in this simulation $\sigma_s \simeq 0.3 - 0.5\sigma_\rho$, however, the infalling satellites themselves are usually in groups with a velocity dispersion greater than σ_s, and hence an effectively more massive halo for friction to act upon. In any case, friction reduces the satellite's infall velocity significantly below that expected for a test particle in the potential.

A small infalling satellite halo will not excite any violent relaxation but will be gradually tidally shredded as it falls towards the center of the cluster. We assume that tidal removal of halo material occurs at the point in its orbit where the cluster density is equal to the density of the relevant region of the infalling halo. Under this assumption, the inner regions of infalling halos at density ρ are able to remain a self-gravitating object that penetrates deeper than $\rho \simeq 100\rho_0$, where infalling material is added to the growing halo (see Bertschinger 1985). For an approximately constant velocity of infall, the binding energy increase is the depth of the potential well at the location of the satellite. The potential energy of the isothermal halo is $W = 2\sigma_\rho^2 \ln(r/r_c) + W_0$. When the satellite material is stripped away, its binding energy E is approximately $W(r)/2$. Therefore, tidal stripping of halo particles at density ρ will occur after the binding energy increases by

$$\Delta E \simeq -\frac{\sigma_\rho^2}{2} \ln\left(\frac{\rho}{100\rho_0}\right) . \tag{2}$$

Figure 5 shows the evolution of binding energy for low-density halos and for the high-density cores of halos. The simple theory outlined above accurately predicts the evolution of binding energy. At $z = 0$ the one-dimensional velocity dispersion of the cluster is 429 km s^{-1}, and for the overdensity 8000 material equation (2) implies an increase in binding energy of (618 km s^{-1})^2, from (1193 km s^{-1})^2 to (1325 km s^{-1})^2, essentially equal to the prediction from equation (2) of 576 km s^{-1})^2. The satellite energies are derived from 37 small, dense cores (a maximum of 77 particles and a minimum of 10) that fall into the cluster fairly late in its development. The larger and initially centrally located halos are excluded.

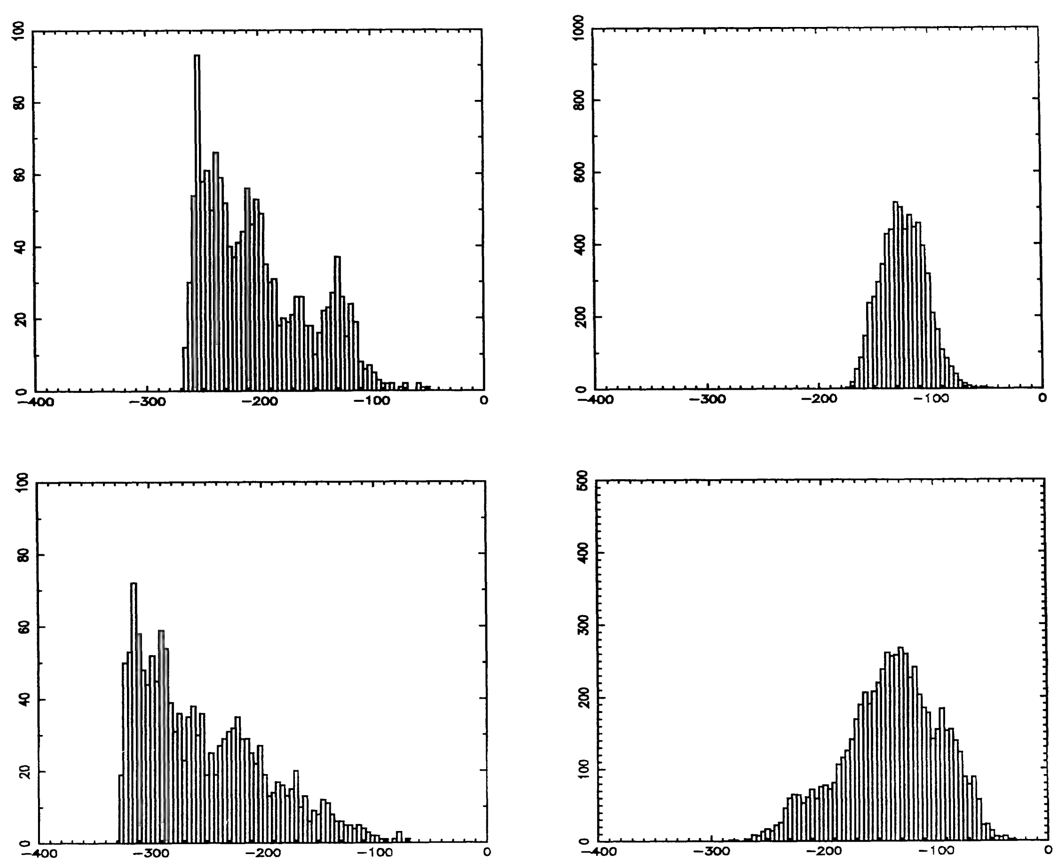

FIG. 5.—The binding energy distributions of particles in groups identified at $z = 3$ which later merge to form the largest cluster. The groups contain at least 10 particles and have $\rho/\rho_0 \geq 8000$ (*left*) and $\rho/\rho_0 \geq 125$ (*right*). The values at $z = 3$ are shown in the top row, and at $z = 0$ in the bottom row. The low-density groups show little change, whereas the high-density groups move to increased binding energy, consistent with dynamical friction followed by tidal disruption. The energy is in units of (74 km s^{-1})^2.

Because the halo infall occurred as relatively small, isolated events, the energies do not change as a result of violent relaxation (Zurek, Quinn, & Salmon 1988). Particles in the core of a halo can lose energy, in sort of a "sacrifice slingshot," which gives the energy to those further out in the halo (Heisler & White 1990). This process aids friction in sinking the cores; however, the energy change in one "sling" expected is $\Delta E \lesssim \sigma_i V \Delta M/M$, where $\Delta M/M$ is the fraction of the satellite's mass sacrificed, where V is the orbital velocity, expected to be less than σ_c, and where σ_i is the internal velocity dispersion of a typical halo, $\simeq 150$ km s^{-1}, leading to a small energy loss compared to that measured. An identical experiment, except using 64 times less particles, found the same magnitude of cooling within the statistical errors, suggesting that two-body relaxation is not an important source of energy transfer. We conclude that the bulk of the core energy decrease is a result of dynamical friction.

5. DISCUSSION

There are two observations which can be nicely understood within a cluster formation model of cosmological infall with friction: the densities of galaxies in the cluster are generally closer to r^{-3} than r^{-2} (e.g., Butcher & Oemler 1984), and their orbits are not primarily radial in the outer virialized regions (Kent & Gunn 1982; The & White 1986; Merrit 1987). If clusters formed by "top-hat" collapse, that is, the near simultaneous collapse of a large nearly uniform density region, then a multitude of simulations and models (e.g., van Albada 1982; Tremaine 1987) have shown that velocity anisotropy increases quickly with radius. Within an infall picture, the material arrives over a long time interval, and there usually is no scale radius that would change the angular momentum of the infalling material; consequently the velocity anisotropy changes little with radius, as is born out by the data in Figure 4. The difficulty with this infall picture is that it then predicts a very shallow density gradient with radius, typically $r^{-9/4}$ (details dependent on the density profile of the initial perturbation, see Gunn 1977), rather than the observed value which approaches r^{-3}. The additional physics of dissipation during infall of a lumpy medium rather than a smooth one does not significantly change the distribution of the bulk of the mass. But the small amount of mass that is centrally located in the dark halos suffers a cumulative energy loss which causes low-velocity dispersion material to be carried deep into the potential well without the normal increase in velocity. The galaxies are a cool subpopulation within the cluster, and consequently have a steeper density profile than the dark matter, more in accord with cluster observations.

Previous investigations have found that dynamical friction certainly causes the galaxies to spiral deeper into the potential well of the cluster or group, but in general they do not find any evidence for a velocity-dispersion difference between the galaxy and dark matter population (Barnes 1984, 1985; Evrard 1986, 1987; West & Richstone 1988). One possibility for the difference is the numbers of particles used, however our simulation repeated with 4096 particles detects a somewhat reduced cooling of the cluster galaxies, the difference being within measurement statistics. To detect a 20% cooling statistically requires $\gtrsim 25$ galaxies which is close to, or exceeds, the numbers used in some of the previous experiments. A cluster of slightly larger mass present in a full cosmological simulation (Carlberg 1991) was analyzed, and found to give $b_v \simeq 0.9$, but with reduced mass resolution and poorer statistics. A simulation detail which is likely quite important is that previous studies have usually been modeled galaxies as one single heavy particle that either has a dark halo attached by hand or only a small amount of time is allowed for the halos to grow (e.g., West & Richstone 1988). The consistent cosmological initial conditions used here started the simulation at $z = 9$ with the full growing mode velocities, which at $z = 0$ will cause a statistically average galaxy to accrete its full $\xi(r) \simeq (10 \text{ Mpc}/r)^{1.8}$ massive dark halo. A small reduction in the correlated mass that is moving coherently with the infalling galaxies will quickly reduce the magnitude of the cooling to insignificant levels in a simulation of cluster collapse.

It is interesting to note the observations of the velocity and density field of the M87 stars as compared to its globular clusters, the stars being cooler with a steeper density profile than the clusters (Mould et al. 1987, 1990), roughly consistent with the values obtained here, provided that the globular clusters were initially in the outer parts of infalling halos, and the stellar body originated from the merging of stars or gas located near their centers. Although this observational evidence for the presence of two kinematic populations might be the result of the dynamical cooling discussed here, this model is designed for clusters of galaxies, and other effects may be present within individual cD galaxies.

6. CONCLUSIONS

A numerical simulation of the formation of a small cluster finds that the particles identified as galaxy orbit tracers have a velocity dispersion significantly less than those in the dominant dark matter. Since galaxy masses orbiting in a 500 km s^{-1} cluster are not subject to strong dynamical friction effects on a dynamical time scale, the presence of a significant velocity bias in the cluster provides strong evidence that the field value for the velocity bias is less than the value 0.8 found in this cluster.

The cluster is created through the cosmological infall of substructure, leading to an approximately isothermal, isotropic density distribution in the dark matter. The luminous parts of galaxies are identified with particles in the high-density $\rho \gtrsim 10^4 \rho_0$ central parts of galaxy-scale halos present at $1 \lesssim z \lesssim 4$, prior to cluster formation. The low-velocity dispersion of the galaxy tracers in the clusters at $z = 0$ is attributed to the action of dynamical friction, primarily acting on the large mass present in the dark halo that initially surrounds each galaxy. Once the low-density outer halo is stripped away (and the central regions shredded in this simulation), the effective mass is greatly reduced, and the friction drops to zero. The process, being effectively dissipative, increases the phase density of the galaxy tracer population in the central part of the cluster, yielding a low-velocity population of galaxies deep in the cluster potential. The galaxy tracers have a radial velocity dispersion which is $b_{vr} = 0.80 \pm 0.05$ of that in the dark matter distribution, and the three-dimensional b_v is approximately 5%–10% less. This estimate of the velocity bias does not account for galaxy merging and dissipation, which can only reduce b_v. The cooled galaxy population has a steeper, denser profile than the dark matter, as expected from equilibrium stellar dynamics, and appears to be roughly in accord with dynamical models of cluster galaxies.

We thank Gus Evrard, the referee, for suggestions which improved the presentation of this material. We greatly acknowledge the support of NSERC of Canada.

REFERENCES

Barnes, J. 1984 MNRAS, 208, 873
———. 1985, MNRAS, 215, 517
Barnes, J. & Hut, P. 1986, Nature, 324, 446
Bertschinger, E 1985, ApJS, 58, 39
Bond, J. R. & Efstathiou, G. E. 1984, ApJ, 285, L45
Butcher, H. & Oemler, A. 1984, ApJ, 285, 426
Carlberg, R. G. 1988, ApJ, 324, 664
———. 1991, ApJ, Feb 1, in press
Carlberg, R. G. & Couchman, H. M. P. 1989, ApJ, 340, 47
Carlberg, R. G., Couchman, H. M. P., & Thomas, P. A. 1990, ApJ, 352, L29
Davis, M. & Peebles, P. J. E. 1983, ApJ, 267, 465
Evrard, A. E. 1986, ApJ, 310, 1
———. 1987, ApJ, 316, 36
———. 1989, ApJ, 341, L71
Filmore, J. A. & Goldreich, P. 1984, ApJ 281, 1
Frenk, C. S., White, S. D. M., Efstathiou, G., & Davis, M. 1990, ApJ, 351, 10
Gott, J. R. & Gunn, J. 1972, ApJ, 176, 1
Gunn, J. 1977, ApJ, 218, 592
Heisler, J. & White, S. D. M. 1990, MNRAS, 243, 199
Kaiser, N. 1984, ApJ, 284, L9
Kaiser, N. & Lahav, O. 1989, MNRAS, 237, 129
Kent, S. & Gunn, J. E. 1982, AJ, 87, 945
Lauer, T. 1988, ApJ, 325, 49
Lynden-Bell, D., Faber, S. M., Burstein, D., Davies, R. L., Dressler, A., Terlevich, R. J., & Wegner, G. 1988, ApJ, 326, 19
Lynden-Bell, D., Lahav, O., & Burstein, D. 1989, MNRAS, 241, 325
Merritt, D. 1987, ApJ, 313, 121
Mould, J. R., Oke, J. B., de Zeeuw, P. T., & Nemec, J. M. 1990, AJ, 99, 1823
Mould, J. R., Oke, J. B., & Nemec, J. M. 1987, AJ, 92, 53
Peebles, P. J. E. 1976, ApJ, 205, L109
Peebles, P. J. E., Daly, R. A., & Juskiewicz, R. 1989, ApJ, 347, 563
Ramella, M., Geller, M. J., & Huchra, J. P. 1989, ApJ, 344, 57
Richstone, D. O. & Malamuth, E. M. 1983, ApJ, 268, 30
The, L. S. & White, S. D. M. 1986, AJ, 92, 1248
Tremaine, S. D. 1987, in IAU Symp 127, Structure and Evolution of Elliptical Galaxies, ed. T. de Zeeuw (Dordrecht: Reidel), p. 367
van Albada, T. S. 1982, MNRAS, 201, 939
West, M. J. & Richstone, D. O. 1988, ApJ, 335, 532
White, S. D. M. 1976, MNRAS, 177, 717
White, S. D. M., Davis, M., Efstathiou, G. & Frenk, C. S. 1987, Nature, 330, 451
White, S. D. M. & Rees, M. J. 1978, MNRAS, 183, 341
Zurek, W. H., Quinn, P. J., & Salmon, J. K. 1988, ApJ, 330, 519